Journal of Zhejiang University SCIENCE A
ISSN 1673-565X (Print); ISSN 1862-1775 (Online)
www.zju.edu.cn/jzus; www.springerlink.com
E-mail: jzus@zju.edu.cn

Development of a linear compressor for two-stage pulse tube cryocoolers

Peng-da YAN†, Wei-li GAO, Guo-bang CHEN

(*Institute of Refrigeration and Cryogenics, Zhejiang University, Hangzhou 310027, China*)

†E-mail: pengda_yan@zju.edu.cn

Received Oct. 23, 2008; Revision accepted Mar. 9, 2009; Crosschecked Sept. 9, 2009

Abstract: A valveless linear compressor was built up to drive a self-made two-stage pulse tube cryocooler. With a designed maximum swept volume of 60 cm^3, the compressor can provide the cryocooler with a pressure volume (PV) power of 400 W. Preliminary measurements of the compressor indicated that both an efficiency of 35%~55% and a pressure ratio of 1.3~1.4 could be obtained. The two-stage pulse tube cryocooler driven by this compressor achieved the lowest temperature of 14.2 K.

Key words: Linear compressor, Linear motor, Pulse tube cryocooler
doi:10.1631/jzus.A0820742 **Document code:** A **CLC number:** TB652

INTRODUCTION

Given the merit of light weight, small size, long life and high efficiency, Stirling-type pulse tube cryocoolers become increasingly practical in their applications for cooling infrared (IR) sensors, high temperature superconducting (HTS) devices, etc. Multi-stage configuration is, however, necessary to meet the requirements for lower temperatures. As a prime mover, the linear compressor plays an essential role in attaining high performance of the pulse tube cryocooler.

Northrop Grumman Space Technology introduced a thermally coupled two-stage Stirling-type pulse tube cryocooler capable of providing a cooling power of 2.25 W at 35 K (Chan, 2003; Nast, 2003; Nguyen, 2004). A lower temperature of 12.8 K was achieved by University of Giessen, Germany in its two-stage Stirling-type pulse tube cryocooler (Tang, 2005). A thermo-acoustically driven two-stage Stirling-type pulse tube cryocooler at Zhejiang University, China reached a temperature as low as 41 K (Tang, 2008). Recently, we built a thermally coupled two-stage pulse tube cryocooler driven by a self-made linear compressor, and obtained the lowest temperature of 14.2 K from the prototype. In this paper, the principle of the compressor and the design of its main parts are discussed; experimental results on the compressor performance are also reported.

STRUCTURE OF THE LINEAR COMPRESSOR

The compressor (outside diameter D=198 mm, length L=550 mm) consists of two linear motors, plate springs and two cylinder-piston sets, which are enclosed in a hermetic casing (Fig.1). The linear motors are of the moving-magnet type, comprising static coil, iron core, and moving magnet. The plate springs keep the moving mass resonating at the operating frequency, so as to avoid excessive reaction current. Two pistons reciprocate synchronously in the opposite direction to generate a nearly sinusoidal pressure wave, which is transferred to the pulse tube cold head through a gas line. Fig.2 shows the two-stage pulse tube cryocooler driven by the linear compressor.

A pressure volume (PV) power of 400 W and a swept volume of 20 cm^3 are required to realize the desired performance of the cryocooler, by means of REGEN 3.2, a numerical model for regenerative heat

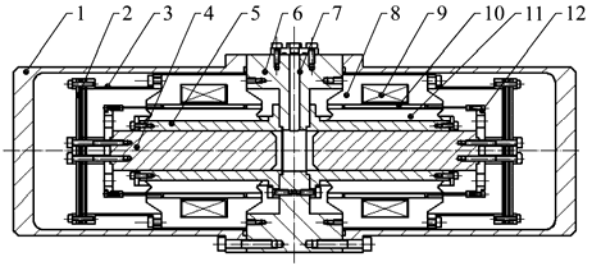

1: casing; 2: plate spring; 3: spring holder; 4: piston; 5: cylinder; 6: base block; 7: output line; 8: outer iron core; 9: coil; 10: magnet; 11: inner iron core; 12: magnet holder

Fig.1 Structure of the linear compressor

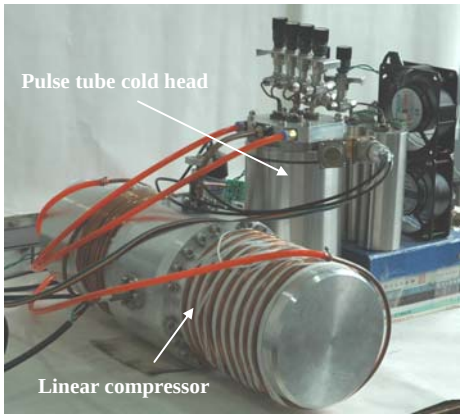

Fig.2 A two-stage pulse tube cryocooler

exchangers (Gary, 2001). In this study, the compressor is designed to have a maximum swept volume of 60 cm^3 and can output a maximum PV power of about 1200 W in its full stroke operation.

LINEAR MOTORS

There are two linear motors in the compressor, arranged in opposite orientations. The moving-magnet motor, as compared to a moving-coil linear motor, needs less magnet mass to produce the same output power with the same efficiency. And it furthermore requires a spring of lower stiffness, since the mass of a moving magnet is much less than that of a moving coil in an equivalent moving-coil motor. However, the moving-magnet motor may bring more eddy current loss and undesirable axial magnetic force when the magnet is not properly centered.

Figs.3 and 4 show the stator and the magnet-piston-spring assembly, respectively. The stator, consisting of iron core and coil, generates an alternating magnetic field when the coil is excited with alternating current. The ring-shape magnet is located in the gas gap constructed by the iron cores. The alternating magnet field drives the magnet and the piston into reciprocating motion. To reduce the eddy current loss, silicon steel laminations are used. Eight laminated stacks are arranged in a star shape around the ring shape coil.

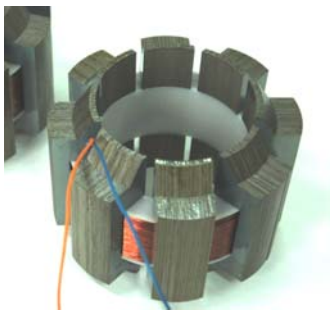

Fig.3 Stator of the linear motor

Fig.4 Magnet-piston-spring assembly

The force that a linear motor can deliver was calculated by a finite element analysis of the electromagnetic field. A portion of the analysis results are given in Fig.5. Fig.5a shows the magnetic flux in the plane of a lamination of the linear motor, while Fig.5b reports the static magnetic force that the linear motor can produce when the magnet is located in each axial position. Besides, the influence of gas gap thickness on the output of the motor is also illustrated. The PV power output of the motor can be estimated by integrating the force along the stroke. The actual PV power should be less than the calculating result, since there is a phase difference between the current and the movement of the magnet in practical operations.

In the primary installation, a copper wire with a diameter of 0.8 mm was used, and the total number of turns was 865. But it was found that the inductance of

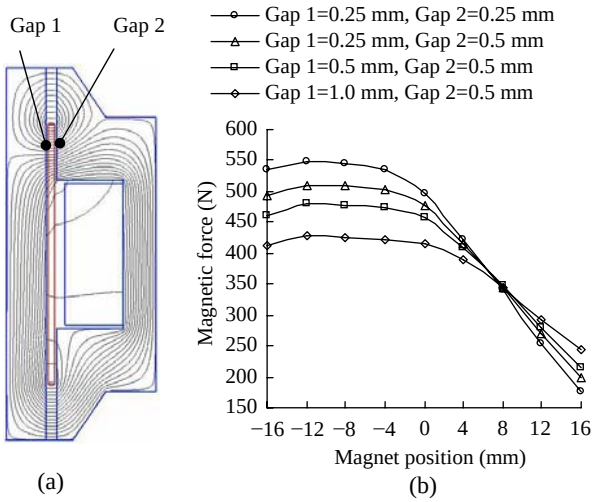

Fig.5 Finite element analysis results of the linear motor. (a) Magnetic flux in the motor; (b) Magnetic forces

the coil was so high that the compressor could not input enough electrical power with an input voltage of about 220 VAC. Then the wire diameter was changed to 1.6 mm, and the number of turns was reduced to 199, so the input electrical power can reach 500~600 W with a voltage of about 100 VAC. The resistance of the coil is 0.58 Ω.

PLATE SPRINGS

To avoid an excessive reaction current and to achieve a higher efficiency, the compressor should be operated at a resonance condition. The resonance frequency is determined by the moving mass and the stiffness of the spring.

The variations in the pulse tube cryocooler such as volume, pressure, mass flow, as well as the movement of the piston exhibit nearly sinusoidal oscillations. The effect of gas pressure on the moving mass can be assumed similar to that of a mechanical spring. So the total elastic coefficient k_m+k_g of the linear motor can be expressed as

$$k_m + k_g = 4\pi^2 m f^2, \quad (1)$$

where k_m represents the axial mechanic stiffness of the mechanical spring, k_g denotes the equivalent elastic coefficient caused by the spring effect of the gas, m is the mass of the moving parts, and f is the operating frequency. The axial stiffness of the mechanical spring is suggested to range between 15%~25% of the total elastic coefficient when plate springs are adopted (Marquardt, 1992).

Plate springs with two spiral arms are used in the compressor, as shown in Fig.6. Plate springs construct the resonating system associated with the moving mass, and suspend one end of the piston within a small radial displacement less than the clearance between the piston and the cylinder. The plate springs own very large radial stiffness, hence there will be no contact if both ends of the piston were suspended. However, suspending both ends of the piston leads to a more complicated structure and a more difficult assembling process. Only one end of the piston is therefore designed to be supported by the plate springs for this present compressor.

A finite element analysis was used to design the plate springs, mainly for calculating the material stress and both axial and radial stiffness. A typical result of the analysis is given in Fig.7. It is found that the maximum stress appears at the edge of spiral arms near the end. A configuration with two wide arms is then selected for its less stress and higher axial stiffness. The plate spring is made of 0.6 mm-thick stainless steel sheet. 8~10 discs of the plate springs are stacked up for one linear motor to meet the requirement of axial stiffness (Fig.6).

Fig.6 Plate spring installed in the compressor

PISTON AND CYLINDER

Considering the requirement of the maximum swept volume of 60 cm^2 and the capacity of the linear motor, the diameter and stroke of the piston are determined as 36 and 30 mm, respectively.

Because the piston does not avoid touching the cylinder, lubrication is necessary. The piston is coated with polytetrafluoroethylene (PTFE), and inner

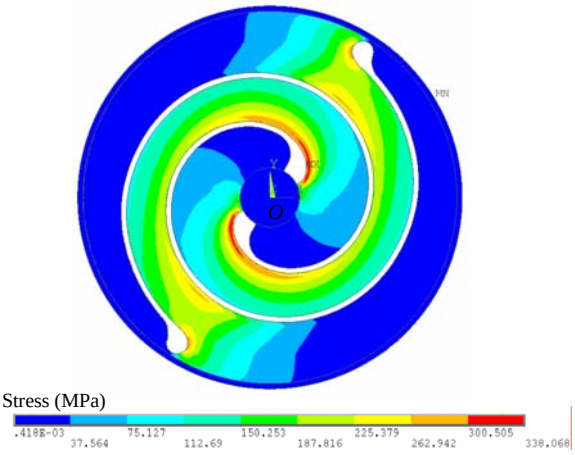

Fig.7 Stress analysis of the plate spring

surface of the cylinder is finely grinded, which significantly reduces the friction resistance and keeps the rubbing under an allowable level.

EXPERIMENTS

In an experiment carried out to test its performance, the compressor was connected with a small gas tank through a needle valve, as shown in Fig.8. Two pressure transducers monitored the pressure waves at the outlet of the compressor and in the gas tank, respectively. The PV power can be calculated from the two pressure wave data. The efficiency is defined as the ratio of PV power to input electric power. The experimental results are shown in Figs.9 and 10.

As shown in Fig.9, the efficiency of the compressor is 30%~45% at an operating frequency of 36 Hz and a mean pressure of 2.0 MPa. The efficiency

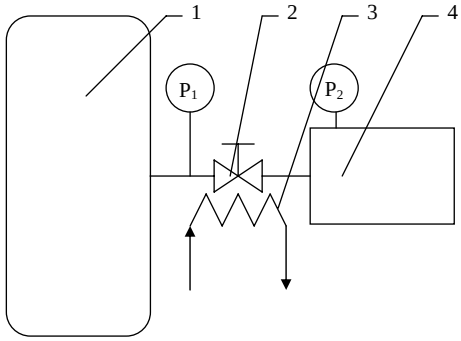

1: compressor; 2: needle valve; 3: water cooler; 4: gas tank; P_1, P_2: pressure transducer

Fig.8 Test setup for compressor efficiency

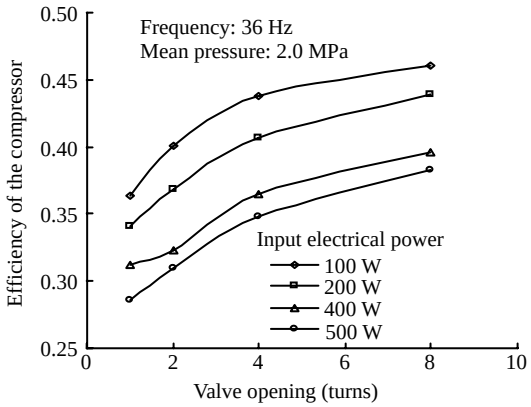

Fig.9 Efficiency of the compressor vs input electrical power and valve opening

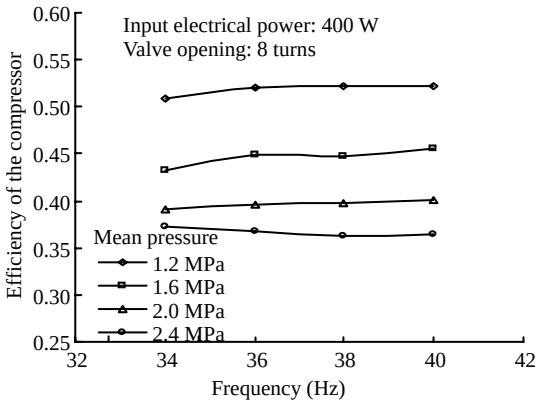

Fig.10 Effect of operating frequency and mean pressure on efficiency of compressor

rises with the increase of the valve opening and declines with the augment of the input electrical power. Obviously, the compressor did not exhibit its best efficiency in this experiment due to the opening limit of the valve. Further measurement will be carried out by checking the displacement of the piston and the output pressure wave when it drives the pulse tube cryocooler, so that the result can be more precise.

Fig.10 shows the effect of operating frequency and mean pressure on the efficiency of the compressor. The efficiency, insensitive to the operating frequency, decreases when the mean pressure increases.

The compressor was then installed to drive a thermally-coupled two-stage pulse tube cold head with a double-inlet phase shifter, as shown in Fig.2. The cryocooler reached the lowest temperature of 14.2 K at the second stage with an input electrical power of about 400 W. More details were reported in (Yan *et al.*, 2008a; 2008b; 2009).

Fig.11 shows the pressure wave at the compressor outlet, when the cryocooler was operating stably at its lowest temperature with a mean pressure of 2.1 MPa. The pressure ratio was usually 1.3~1.4 during the stable operation, while remaining as high as 1.5 when the cryocooler was started.

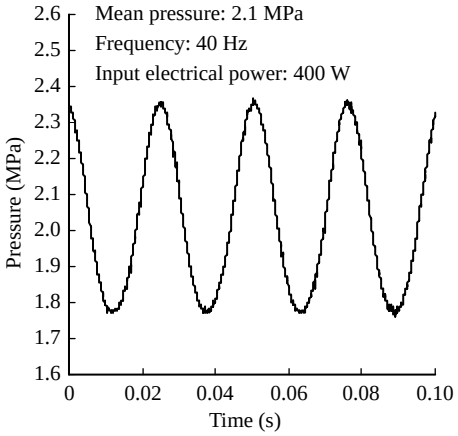

Fig.11 Pressure wave at the outlet of the compressor

Table 1 shows the typical operating parameters of the compressor, when the cryocoole reached its lowest temperature.

Table 1 Typical operating parameters of the compressor

p_m (MPa)	r_p	f (Hz)	V (V)	I (A)	P_e (W)	cosφ
2.1	1.33	40	86.6	11.48	400	0.405

p_m: mean pressure; r_p: pressure ratio; f: frequency; V: voltage; I: current; P_e: electrical power; cosφ: power factor

The power factor, cosφ, where φ is the angle between current and voltage, is an important parameter to inspect the running condition of the compressor. The higher power factor indicates that the compressor operates at a frequency closer to its resonance frequency. Fig.12 shows the effect of operating frequency on the power factor. The peak of each curve indicates the resonance frequency when the compressor operates at the corresponding mean pressure. Then a curve of resonance frequency versus mean pressure can be traced from the data of Fig.12, as shown in Fig.13. It shows that the resonance frequency increases with the mean pressure, and this compressor has resonance frequencies between 33 and 40 Hz, when the cryocooler is charged with a pressure between 1.3 and 2.5 MPa.

Figs.14 and 15 show the temperatures that each stage has reached, when the cryocooler operates at frequencies between 30 and 50 Hz. The temperatures of both stages are almost constant in the frequency range below 40 Hz, and they increase with the frequency. The lowest temperature of 14.2 K can be achieved by this cryocooler.

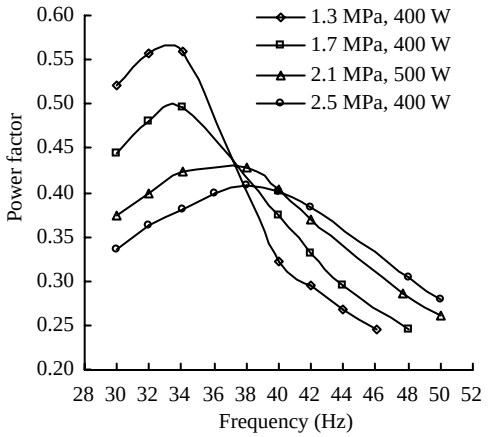

Fig.12 Power factor vs operating frequency

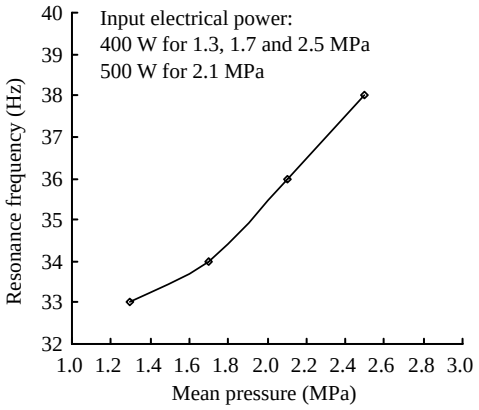

Fig.13 Resonance frequency vs mean pressure

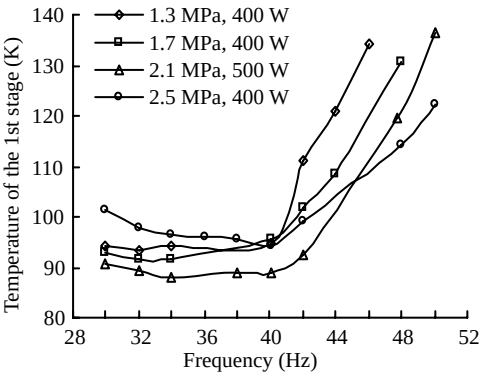

Fig.14 Effect of operating frequency on refrigeration temperature of the 1st stage

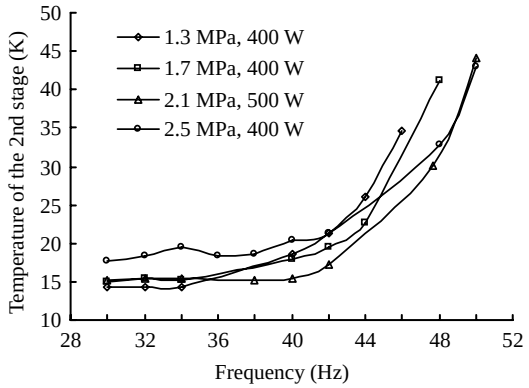

Fig.15 Effect of operating frequency on refrigeration temperature of the 2nd stage

CONCLUSION

The design, manufacture and experimental testing of a linear compressor are discussed. The linear motor is of the moving-magnet type, which was designed by means of the finite element method. The plate spring has also been optimized by the finite element method.

With a maximum swept volume of 60 cm^3, the compressor was designed to output enough PV power more than 400 W to drive the pulse tube cryocooler. It generated a pressure ratio of 1.3~1.4 when driving a two-stage pulse tube cryocooler, and successfully obtained a refrigeration temperature as low as 14.2 K. The PV power measurement of the compressor indicated that an efficiency of about 35%~55% was achieved.

Further researches are needed to improve the compressor efficiency and satisfy the requirement for high performance pulse tube cryocoolers.

References

Chan, C.K., Nguyen, T., Jaco, C., Tomlinson, B.J., Davis, T., 2003. High Capacity Two-Stage Pulse Tube Cooler. Cryocoolers 12, Kluwer Academic/Plenum Publishers, New York, p.219-224.

Gary, J., O'Gallagher, A., Radebaugh, R., Marquardt, E., 2001. REGEN 3.2: User Manual. National Institute of Standards and Technology (NIST) of USA, Boulder, Colorado.

Marquardt, E., Radebaugh, R., Kittel, P., 1992. Design Equations and Scaling Laws for Linear Compressors with Flexure Springs. Cryocoolers 7, ICC Press, Boulder, Colorado, p.783-804.

Nast, T.C., Olson, J., Evtimov, B., 2003. Development of a Two-Stage Pulse Tube Cryocooler for 35 K. Cryocooler 12, Kluwer Academic/Plenum Publishers, New York, p.213-218.

Nast, T.C., Olson, J., Roth, E., Evtimov, B., Frank, D., Champagne, P., 2007. Development of Remote Cooling Systems for Low Temperature Space Borne Systems. Cryocoolers 14, ICC Press, Boulder, Colorado, p.33-40.

Nguyen, C., Yeckley, A., Culler, A., Haberbusch, M., Radebaugh, R., 2004. Hydrogen/Oxygen Propellant Densifier Using a Two-Stage Pulse Tube Cryocooler. Advances in Cryogenic Engineering 49(B), Plenum Press, New York, p.1703-1709.

Nguyen, T., Colbert, R., Durand, D., Jaco, C., Michaelian, M., Tward, E., 2007. 10 K Pulse Tube Cooler. Cryocoolers 14, ICC Press, Boulder, Colorado, p.27-31.

Olson, J., Nast, T.C., Evtimov, B., 2003. Development of a 10 K Pulse Tube Cryocooler for Space Applications. Cryocoolers 12, Kluwer Academic/Plenum Publishers, New York, p.241-246.

Tang, K., Chen, G.B., Thummes, G., 2005. 13 K thermally coupled two-stage Stirling-type pulse tube refrigerator. *Chinese Science Bulletin*, **50**(16):1814-1816. [doi:10.1360/982005-750]

Tang, K., Huang, Z., Lin, X., Xiang, J., Chen, G., 2008. Refrigeration characteristic experiment in 40 K region of a two-stage pulse tube cryocooler driven by a standing wave thermoacoustic engine. *Cryogenic Engineering*, **4**:1-5 (in Chinese).

Yan, P.D., Chen, G.B., Dong, J.J., Gao, W.L., 2008a. Improvement of a Stirling type two stage pulse tube cryocooler. *Cryogenic Engineering*, **5**:7-10 (in Chinese).

Yan, P.D., Chen, G.B., Dong, J.J., Gao, W.L., 2008b. Study of a Stirling type two stage pulse tube cryocooler. *Cryogenic Engineering*, **3**:1-3 (in Chinese).

Yan, P.D., Chen, G.B., Dong, J.J., Gao, W.L., 2009. 15 K two-stage Stirling-type pulse tube cryocooler. *Cryogenics*, **49**(2):103-106. [doi:10.1016/j.cryogenics.2008.10.011]